11-2007

Stability Issues for Gas-Liquid Flows in Bubble Columns

Deify Law
Iowa State University

Francine Battaglia
Virginia Polytechnic Institute and State University

Theodore J. Heindel
Iowa State University, theindel@iastate.edu

Proceedings of IMECE2007
2007 ASME International Mechanical Engineering Congress and Exposition
November 11-15, 2007, Seattle, Washington, USA

IMECE2007-43517

STABILITY ISSUES FOR GAS-LIQUID FLOWS IN BUBBLE COLUMNS

Deify Law
Mechanical Engineering Department
Iowa State University
Ames, Iowa 50011

Francine Battaglia*
Mechanical Engineering Department
Virginia Polytechnic Inst & State Univ
Blacksburg, Virginia 24061

Theodore J. Heindel
Mechanical Engineering Department
Iowa State University
Ames, Iowa 50011

ABSTRACT

In the present work, gas-liquid flow dynamics in a bubble column are simulated with CFDLib using an Eulerian-Eulerian ensemble-averaging method in a two dimensional Cartesian system. The time-averaged gas holdup simulations are compared to experimental measurements of a cylindrical bubble column performed by Rampure et al. [1]. Numerical predictions are presented for the time-averaged gas holdup at various axial heights as a function of radial position. The effects of grid resolution, bubble pressure model, and drag coefficient models on the numerical predictions are examined. The bubble pressure model is reported to account for bubble stability, thus providing physical solutions. The objectives are to obtain grid-independent numerical solutions to resolve unphysical results observed in FLUENT with increasing grid resolutions [2], and to validate computational fluid dynamics simulations with experimental data to demonstrate the use of numerical simulations as a viable design tool for gas-liquid bubble column flows.

NOMENCLATURE

C_D	drag coefficient
d_d	bubble diameter (m)
$G_{k,c}$	production of turbulent kinetic energy (m^2/s^3)
g	acceleration due to gravity (m/s^2)
K_{ip}	interfacial momentum exchange term (kg/m^3)
k_c	turbulent kinetic energy per unit mass (m^2/s^2)
p	pressure (Pa)
Re	Reynolds number
u_p	velocity (m/s)

Greek Symbols

α_p	holdup
ε_c	turbulent energy dissipation rate for continuous phase (m^2/s^3)
$\mu_{t,c}$ (Pa-s)	turbulent dynamic viscosity for continuous phase
II_{kc}, $II_{\varepsilon c}$	interfacial turbulent momentum transfer
ρ_p	density (kg/m^3)
σ_k, σ_ε	turbulent Schmidt number for k and ε, respectively
τ_p	effective stress (N/m^2)

Subscripts

c	continuous phase
d	dispersed phase
p	represents either continuous or dispersed phase

INTRODUCTION

Bubble column reactors are widely used in the chemical industry due to their excellent heat and mass transfer characteristics, simple construction, and ease of operation. As reactors, they are used in a variety of chemical processes, such as Fischer-Tropsch synthesis, manufacture of fine chemicals, oxidation reactions, alkylation reactions, effluent treatment, coal liquefaction, fermentation reactions [3], and production of biobased fuel from biorenewable resources. Bubble column hydrodynamics are studied experimentally and computationally for scale-up and design considerations. The performance of bubble column reactors depends on the gas holdup, bubble size, bubble rise velocity, bubble-bubble

* Corresponding author; Email: battagliaf@asme.org

interactions, and mixing rate [4, 5]. Full-scale experimentation in bubble columns is expensive; a more cost-effective approach to exploring these reactors is by using validated computational fluid dynamics (CFD) models.

Numerical simulations of bubble columns either employing Eulerian-Eulerian models [1, 3, 6-8], Eulerian-Lagrangian models [9-11], or volume of fluid (VOF) [12] methods were surveyed. The Eulerian-Eulerian model treats dispersed (gas bubbles) and continuous (liquid) phases as interpenetrating continua, and describes the motion for gas and liquid phases in an Eulerian frame of reference. Sokolichin and Eigenberger [6], Pan et al. [7], and Monahan et al. [8] performed two-dimensional (2D) simulations of gas-liquid flows for a rectangular bubble column using an Eulerian-Eulerian approach. Sokolichin and Eigenberger [6] and Pan et al. [7] predicted time-averaged axial liquid velocity results and reported that the liquid primarily traveled up the column center and reduced gas holdup with liquid downflow at the walls. Monahan et al. [8] demonstrated that the two-fluid model can predict flow transitions in bubble columns successfully. Other investigators such as Rampure et al. [1], who conducted three-dimensional (3D) simulations, and Sanyal et al. [3], who conducted axisymmetric simulations of a cylindrical bubble column reactor, used the Eulerian-Eulerian method as well. It should be noted that both Rampure et al. [1] and Sanyal et al. [3] conducted experiments in addition to numerical simulations and the time-averaged gas holdup simulations compared qualitatively with the experiments.

In the Eulerian-Lagrangian model, the continuous phase is described in an Eulerian representation while the dispersed phase is treated as discrete bubbles and each bubble is tracked by solving the equations of motion for individual bubbles. Delnoij et al. [9-11] applied an Eulerian-Lagrangian method to simulate detailed bubble-bubble interactions along with interfacial forces in the laminar bubbly flow regime. They predicted a clear bubble plume and a time-dependent, multiple staggered vortex mode of circulation that characterizes the liquid bed of the bubble column. The computed flow structure qualitatively compared with the experimentally observed flow patterns.

The VOF method solves the instantaneous Navier-Stokes equations to obtain the gas and liquid flow field with an extremely high spatial resolution. The evolution of the gas-liquid interface is tracked using a volume-tracking scheme. Lin et al. [12] used the VOF method to provide time-dependent behavior of a dispersed bubbling flow and to account for the coupling effects of the pressure field and the liquid velocity on the bubble motion based on their 2D bubble column simulations. The computational results indicated the unsteady nature of the flow due to the coupling effects of the pressure field, liquid velocity, and bubble motion. The numerical results compared well both qualitatively and quantitatively with the experiments [12].

The main advantage of the Eulerian-Lagrangian formulation comes from the fact that each individual bubble is modeled as it flows through the column. This allows for a direct consideration of additional effects related to bubble-bubble and bubble-liquid interaction. Mass transfer with and without chemical reaction, bubble coalescence and redispersion can, in principle, be added directly to an Eulerian-Lagrangian hydrodynamic model. The Eulerian-Lagrangian approach, which requires tracking the dynamics of each bubble, is usually applied to cases with low superficial gas velocity due to computer limitations. On the other hand, the Eulerian-Eulerian method is often used because memory storage requirements and demand of computer power depend only on the number of computational cells considered instead of the number of bubbles. The Eulerian-Eulerian approach can be applied to cases for low and high superficial gas velocities. The disadvantage of using the Eulerian-Eulerian method is that the bubble-bubble and bubble-liquid interaction cannot be considered as straightforward as the Eulerian-Lagrangian method. The VOF method is the most detailed model used to advance the gas-liquid interface through the flow field in an Eulerian mesh and does not require any empirical constitutive equations. However, the VOF method is limited to a small number of bubbles, such as less than 10 bubbles in the flow field, due to computational limitations. In most industrial applications, high superficial gas velocity is used and therefore the Eulerian-Eulerian method is preferred [7]

Law et al. [2] studied bubble column hydrodynamics computationally using the Eulerian-Eulerian method formulated in FLUENT. Unphysical results were observed with increasing grid resolutions using FLUENT, therefore prohibiting a conclusive grid resolution study. An alternate multiphase FORTRAN code, CFDLib, developed at Los Alamos National Laboratory, is tested in the present work. The hypothesis is that a bubble pressure (BP) model will provide numerical and bubble phase stabilities to resolve the flow field correctly. Monahan et al. [8] reported that the BP model provides a uniform time-averaged gas holdup profile across the bubble column in the low superficial gas velocity flow regime.

In the present work, the gas-liquid flow dynamics in the bubble column are simulated using CFDLib in two-dimensional Cartesian coordinates. The time-averaged gas holdup results are compared to the experimental measurements of a cylindrical bubble column performed by Rampure et al. [1]. Numerical predictions are presented for the time-averaged gas holdup at various axial heights as a function of radial position. The effects of grid resolution, bubble pressure model, and drag coefficient model on the numerical predictions are also examined. The objectives are to obtain grid-independent numerical solutions and to validate the CFD simulations with the published experimental data in order to demonstrate the use of numerical simulations as a viable design tool.

NUMERICAL FORMULATION

Governing Equations

CFDLib, a FORTRAN code developed at Los Alamos National Laboratory, uses a finite-volume technique to integrate the time-dependent equations of motion that govern multiphase flows. The code is based on an Arbitrary Lagrangian-Eulerian (ALE) scheme as described by [13]. The name ALE refers to the flexibility of the scheme, which allows for the mesh either to be moved along with the fluid (Lagrangian), to remain in a fixed position (Eulerian), or to be moved in another fashion as selected by the user. The ALE scheme is designed to handle flows at any flow speed, including incompressible and hypersonic flows, and it allows for multiphase calculations for an arbitrary number of fluid fields. The two-fluid Eulerian-Eulerian model is employed to represent each phase as interpenetrating continua and the conservation equations for mass and momentum for each phase are ensemble-averaged. The subscript c refers to the continuous (liquid water) phase and the subscript d refers to the dispersed (air bubble) phase. The continuity equations for each phase, neglecting mass transfer, are:

$$\frac{\partial}{\partial t}(\alpha_c \rho_c) + \nabla \cdot (\alpha_c \rho_c \vec{u}_c) = 0 \tag{1}$$

$$\frac{\partial}{\partial t}(\alpha_d \rho_d) + \nabla \cdot (\alpha_d \rho_d \vec{u}_d) = 0 \tag{2}$$

The momentum equations for each phase are:

$$\frac{\partial}{\partial t}(\alpha_c \rho_c \vec{u}_c) + \nabla \cdot (\alpha_c \rho_c \vec{u}_c \vec{u}_c) = -\alpha_c \nabla p + \nabla \cdot \bar{\bar{\tau}}_c + \sum_{i=c,d} \vec{K}_{ic}(\vec{u}_i - \vec{u}_c) + \vec{F}_{vm} + \rho_c \alpha_c \vec{g} \tag{3}$$

$$\frac{\partial}{\partial t}(\alpha_d \rho_d \vec{u}_d) + \nabla \cdot (\alpha_d \rho_d \vec{u}_d \vec{u}_d) = -\alpha_d \nabla p + \nabla \cdot \bar{\bar{\tau}}_d + \sum_{i=c,d} \vec{K}_{id}(\vec{u}_i - \vec{u}_d) - \vec{F}_{vm} + \rho_d \alpha_d \vec{g} \tag{4}$$

The terms on the right hand side of Eqs. (3) and (4) represent, from left to right, the pressure gradient, effective stress, interfacial momentum exchange (drag and virtual mass forces), and the gravitational force. The closures for turbulence modeling and interfacial momentum exchange are discussed next.

Turbulence Modeling

Turbulence contributions for the continuous and the dispersed phases are modeled through a set of modified standard k-ε equations supplemented with extra terms that include interfacial turbulent momentum transfer [14, 15]. The modified k-ε equations for the liquid phase are:

$$\frac{\partial}{\partial t}(\alpha_c \rho_c k_c) + \nabla \cdot (\alpha_c \rho_c k_c \vec{u}_c) = \nabla \cdot \left(\alpha_c \frac{\mu_{t,c}}{\sigma_k} \nabla k_c \right) + \alpha_c G_{k,c} - \alpha_c \rho_c \varepsilon_c + \alpha_c \rho_c II_{kc} \tag{5}$$

$$\frac{\partial}{\partial t}(\alpha_c \rho_c \varepsilon_c) + \nabla \cdot (\alpha_c \rho_c \varepsilon_c \vec{u}_c) = \nabla \cdot \left(\alpha_c \frac{\mu_{t,c}}{\sigma_\varepsilon} \nabla \varepsilon_c \right) + \alpha_c \frac{\varepsilon_c}{k_c}(C_{1\varepsilon} G_{k,c} - C_{2\varepsilon} \rho_c \varepsilon_c) + \alpha_c \rho_c II_{\varepsilon c} \tag{6}$$

where

$$\mu_{t,c} = \rho_c C_\mu \frac{k^2}{\varepsilon} \tag{7}$$

$$G_{k,c} = \mu_{t,c}(\nabla \vec{u}_c + (\nabla \vec{u}_c)^T) : \nabla \vec{u}_c \tag{8}$$

The variables II_{kc} and $II_{\varepsilon c}$ are the interfacial turbulent momentum transfer terms that are derived from the instantaneous continuous liquid phase and involves the continuous-dispersed velocity covariance. Similar formulations can be derived for the dispersed gas phase [12]. Equations (7) and (8) are the closure models for the production of turbulent kinetic energy $G_{k,c}$ and turbulent viscosity $\mu_{t,c}$ of the continuous phase. The turbulent parameters are set using standard empirical values for k-ε turbulence modeling where $C_{1\varepsilon} = 1.44$, $C_{2\varepsilon} = 1.92$, $C_\mu = 0.09$, $\sigma_k = 1.0$, and $\sigma_\varepsilon = 1.3$.

Interfacial Momentum Exchange

The interfacial momentum exchange terms in the momentum conservation equations for each phase consist of drag and virtual mass force terms. The drag force for the gas and liquid, is modeled, respectively, as:

$$\vec{K}_{cd}(\vec{u}_c - \vec{u}_d) = \frac{3}{4} \rho_c \alpha_d \alpha_c \frac{C_D}{d_d} |\vec{u}_c - \vec{u}_d| (\vec{u}_c - \vec{u}_d)$$

$$\vec{K}_{dc}(\vec{u}_d - \vec{u}_c) = \frac{3}{4} \rho_c \alpha_d \alpha_c \frac{C_D}{d_d} |\vec{u}_d - \vec{u}_c| (\vec{u}_d - \vec{u}_c) \tag{9}$$

where C_D is the drag coefficient. The virtual mass force $\vec{F}_{vm}$ is modeled as:

$$\vec{F}_{vm} = 0.5 \alpha_d \rho_c \left(\frac{d\vec{u}_c}{dt} - \frac{d\vec{u}_d}{dt} \right) \tag{10}$$

where the coefficient of 0.5 is used for a spherical bubble.

Drag Coefficient Model

Two drag coefficient models are used for gas-liquid flows. The drag coefficient model proposed by Schiller and Naumann [16] is:

$$C_D = \begin{cases} 24(1+0.15\,\mathrm{Re}^{0.687})/\mathrm{Re} & \mathrm{Re} \le 1000 \\ 0.44 & \mathrm{Re} > 1000 \end{cases} \quad (11)$$

where Re is the bubble Reynolds number based on a characteristic (effective) bubble diameter and the liquid properties. Another drag coefficient relation proposed by Wang-VanderHeyden [17] is expressed by:

$$C_D = 0.5 + \frac{24}{\mathrm{Re}} + \frac{6}{1+\sqrt{\mathrm{Re}}} \quad (12)$$

Bubble Pressure Model

The bubble pressure (BP) model represents the transport of momentum arising from bubble-velocity fluctuations, collisions, and hydrodynamic interactions. The BP model is reported in the literature to play an important role in bubble-phase stability [18]. Biesheuvel and Gorissen [19] proposed a bubble pressure model of the form:

$$P_d = \rho_c C_{BP} \alpha_d (u_d - u_c)(u_d - u_c)\left(\frac{\alpha_d}{\alpha_{dcp}}\right)\left(1 - \frac{\alpha_d}{\alpha_{dcp}}\right) \quad (13)$$

The gradient of Eq. (13) is added into the right hand side of the gas momentum equation (4). A positive value of $dP_d/d\alpha_d$ acts as a driving force for bubbles to move from areas of higher α_d to areas of lower α_d, and facilitates stabilization of the bubbly-flow regime. The virtual mass coefficient C_{BP} of an isolated spherical bubble is 0.5. The bubble pressure is proportional to the slip velocity and the gas holdup. The gas holdup at close packing α_{dcp} is set equal to 1.0 in this study.

SIMULATION CONDITIONS

Simulations are performed to match the experimental conditions of Rampure et al. [1] for a bubble column that is 2.0 m high with a 0.2 m diameter, as shown in Fig. 1. The static water height in the column is 1.0 m. Air flows uniformly through the bottom of the column at 0.1 m/s. The geometry in Fig. 1 is modeled as a 2D slice through the centerplane of the cylinder in Cartesian coordinates. The Marker and Cell (MAC) method has been selected in CFDLib to solve the incompressible gas-liquid two phase flow. A velocity inlet boundary condition is used to introduce gas flow uniformly at the bottom of the bubble column. The no-slip boundary condition is applied for both phases at the walls and ambient pressure is specified at the top of the domain. An effective bubble size of 0.5 cm is used to represent the dispersed gas phase. The convergence criterion is set to 1×10^{-8} for all dependent variables. All the simulations use a fixed time step of 0.01 s to march the solution forward and the results are time-averaged from 20 to 90 s, which includes 7000 time realizations.

RESULTS AND DISCUSSION

Grid Resolution Study

Six different grid resolutions are tested using CFDLib to simulate the 2D representation of the domain in Fig. 1. The number of computational cells along the horizontal and vertical directions is increased while maintaining a square computational cell; a summary of grid resolutions is presented in Table 1. The effects of grid resolution on the numerical predictions of the time-averaged gas holdup were examined and compared to previous results by the authors using FLUENT [2]. For both the FLUENT and CFDLib simulations, Schiller-Naumann drag coefficient model is used.

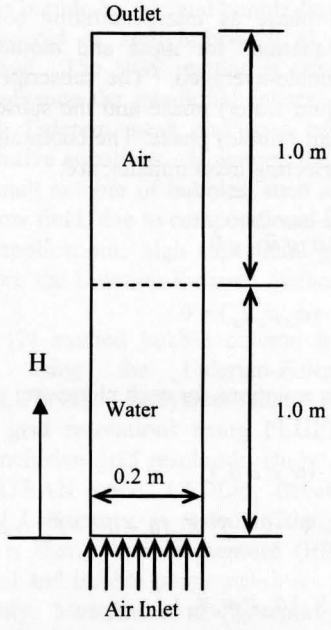

Figure 1. SCHEMATIC OF THE DOMAIN USED IN THE SIMULATIONS OF AN AIR-WATER BUBBLE COLUMN.

Table 1. CELL NUMBER AND SIZE *X*- & *Y*-DIRECTIONS.

# cells ($x \times y$)	$\Delta x = \Delta y$ (cm)
10 × 100	2.00
15 × 150	1.33
20 × 200	1.00
30 × 300	0.66
40 × 400	0.50
60 × 600	0.33

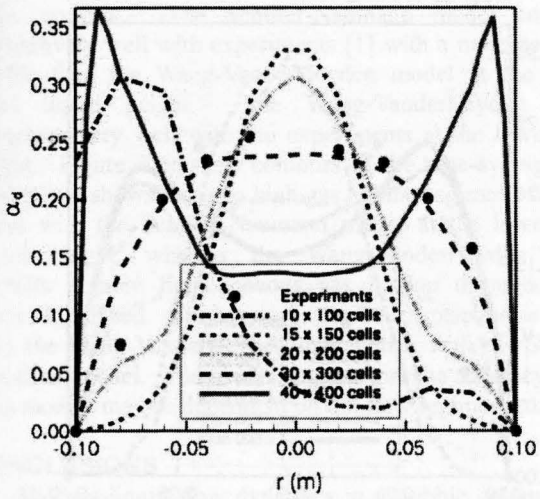

(a) H=0.15 m

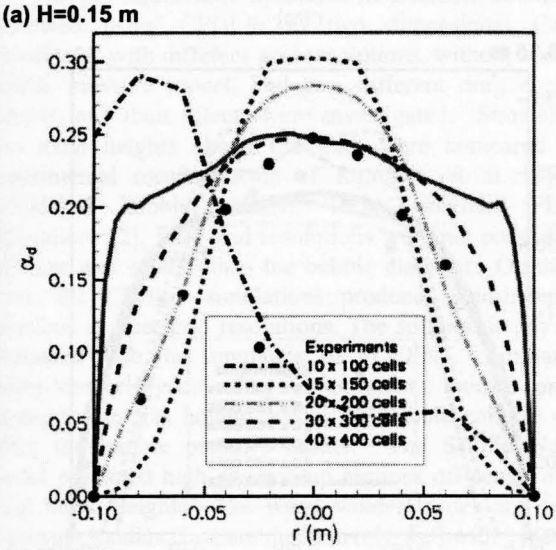

(b) H=0.65 m

Figure 2. TIME-AVERAGED GAS HOLDUP VERSUS RADIAL POSITION COMPARING FLUENT SIMULATIONS [2] USING DIFFERENT GRID RESOLUTIONS WITH EXPERIMENTAL DATA [1] AT HEIGHTS OF (a) 0.15 m AND (b) 0.65 m.

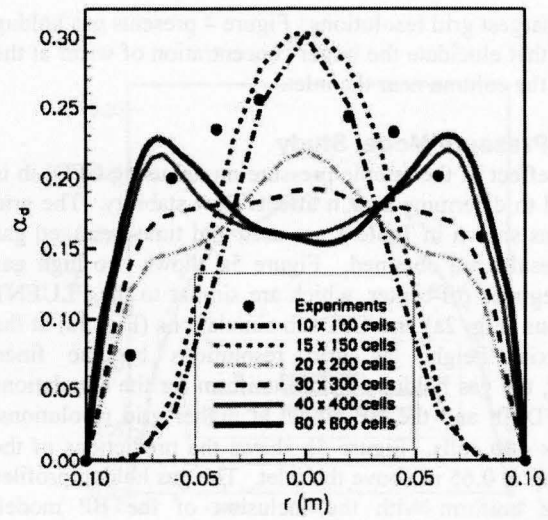

(a) H=0.15 m

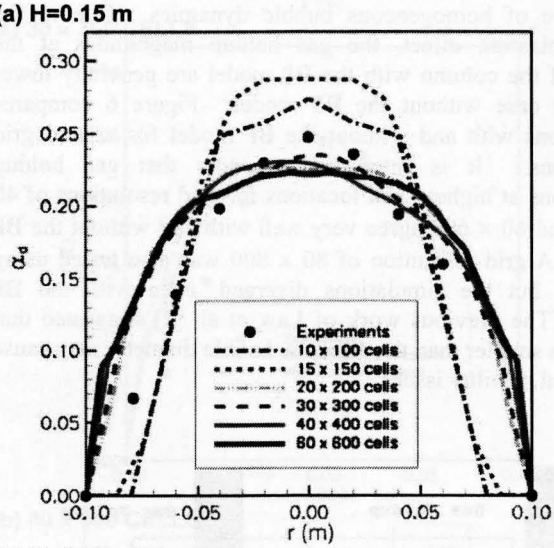

(b) H=0.65 m

Figure 3. TIME-AVERAGED GAS HOLDUP VERSUS RADIAL POSITION COMPARING CFDLIB SIMULATIONS USING DIFFERENT GRID RESOLUTIONS WITH EXPERIMENTAL DATA [1] AT HEIGHTS OF (a) 0.15 m AND (b) 0.65 m.

Figure 2 shows the predictions of the time-averaged gas holdup using FLUENT for axial locations of 0.15 m and 0.65 m above the distributor plate [2]. Results from the experiments of Rampure et al. [1] are compared to the simulations for varying grid resolution. FLUENT best predicts the experimental data using the 30 × 300 grid resolution whereas the 10 × 100 grid resolution gives completely unphysical flow dynamics that fail to capture experimental phenomena. For the cases of 15 × 150 and 20 × 200 cells, the numerically predicted values overestimate the maximum gas volume fraction at the centerline and underestimate it toward the walls. Grid independent solutions of gas-liquid bubble column flow were not obtained [2]. FLUENT was not able to satisfy convergence for the resolution of 60 × 600 cells, even with a small time step size of 0.0001 s. The radial profiles for all predicted time-averaged gas holdup values using FLUENT are generally symmetric, except for the lowest cell resolution case of 10 × 100 cells.

Similar trends are observed from the CFDLib simulations, shown in Figure 3 for axial heights of 0.15 m and 0.65 m. At low axial heights, both FLUENT (Fig. 2a) and CFDLib (Fig. 3a) overpredict the gas holdup near the centerline for low grid resolutions, e.g., 15 × 150 grid cells. For higher grid resolutions such as 40 × 400 cells, both codes predict two local maxima for gas holdup. The gas holdup predictions using CFDLib at 0.65 m (Fig. 3b) indicate grid convergence

for the 3 largest grid resolutions. Figure 4 presents gas holdup contours that elucidate the larger concentration of water at the center of the column near the inlet.

Bubble Pressure Model Study

The effect of the bubble pressure model using CFDLib is examined to determine how it affects flow stability. The grid resolutions shown in Table 1 are used and time-averaged gas holdup results are obtained. Figure 5a shows two high gas holdup regimes off-center, which are similar to the FLUENT simulations (Fig. 2a) and CFDLib simulations (Fig. 3a) at the lower axial height, as grid resolutions become finer. However, the gas holdup is more uniform for the simulations using CFDLib and the BP model at higher grid resolutions, e.g., 40 × 400 cells. Figure 5b shows the predictions of the gas holdup at 0.65 m above the inlet. The gas holdup profiles are more uniform with the inclusion of the BP model, indicative of homogeneous bubble dynamics. Due to the homogenization effect, the gas holdup magnitudes at the center of the column with the BP model are generally lower than the case without the BP model. Figure 6 compares simulations with and without the BP model for several grid resolutions. It is interesting to note that gas holdup predictions at higher axial locations for grid resolutions of 40 × 400 and 60 × 600 agree very well with and without the BP model. A grid resolution of 80 × 800 was also tested using CFDLib but the simulations diverged, even with the BP model. The previous work of Law et al. [2] suggested that cell sizes smaller than the effective bubble diameter may cause numerical stability issues.

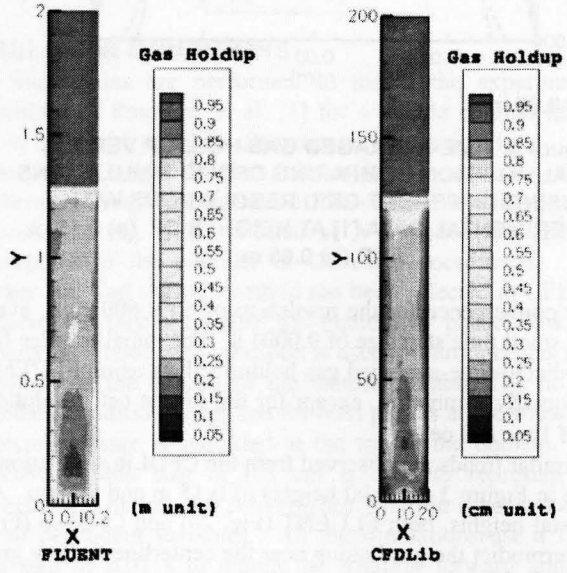

Figure 4. TIME-AVERAGED GAS HOLDUP CONTOUR PLOTS COMPARING FLUENT WITH CFDLIB SIMULATIONS USING 40 × 400 CELLS.

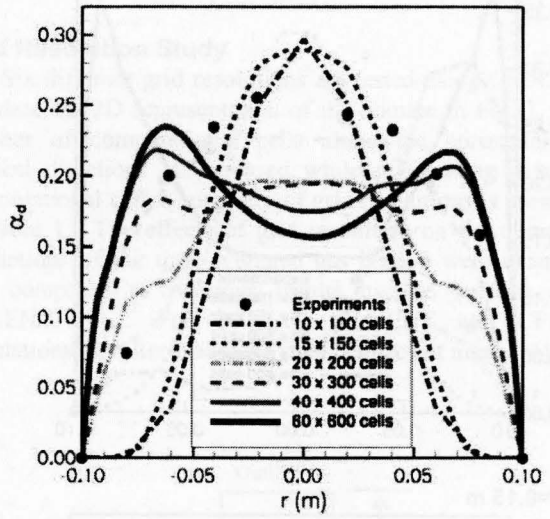

(a) H= 0.15 m

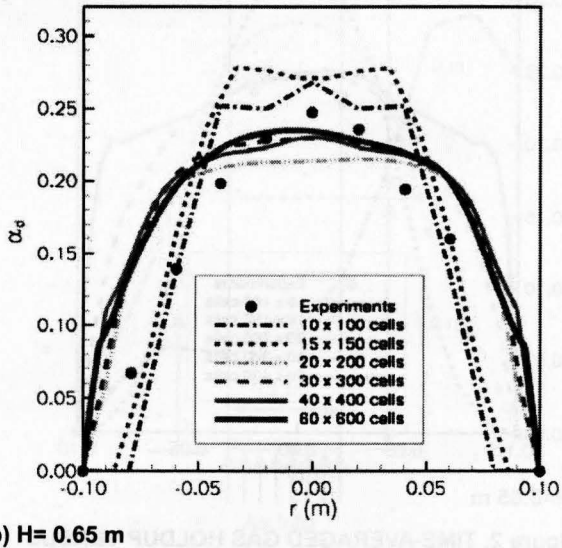

(b) H= 0.65 m

Figure 5. TIME-AVERAGED GAS HOLDUP VERSUS RADIAL POSITION USING THE BUBBLE PRESSURE MODEL COMPARING CFDLIB SIMULATIONS WITH EXPERIMENTAL DATA [1] AT (a) 0.15 m AND (b) 0.65 m.

Drag Coefficient Model Study

Drag coefficient models are investigated to determine the effect on the gas holdup. The grid resolution for this study uses 30 × 300 grid cells and the bubble pressure model is not employed. Figure 7 presents the predicted time-averaged gas holdup for the Wang-VanderHeyden and Schiller-Naumann models, respectively. In general, the time-averaged gas holdup profiles are more homogeneous using the Wang-VanderHeyden model as compared to the Schiller-Naumann model at 0.65 m axial height. It is interesting to note that the effect of Wang-VanderHeyden model is similar to the effect of the bubble pressure model in that the gas holdup profile is

more uniform. The Schiller-Naumann model compares qualitatively well with experiments [1] with a more parabolic profile than the Wang-VanderHeyden model at the higher axial liquid height. The Wang-VanderHeyden model compares very well with the experiments at the lower axial height. Figure 8 presents contours of the time-averaged gas holdup and shows that two high gas holdup regimes off-center occur with the Schiller-Naumann model at the lower axial liquid height, whereas the Wang-VanderHeyden model predicts a more homogeneous gas holdup throughout the entire liquid bed. Furthermore, the bed expansion is higher with the Wang-VanderHeyden model than with the Schiller-Naumann model. The results suggest that the accuracy of the drag models may be dependent on the flow regime.

CONCLUSIONS

The gas-liquid flow dynamics in a bubble column were simulated using CFDLib in two dimensional Cartesian coordinates with different grid resolutions, without and with a bubble pressure model, and two different drag coefficient models, and their effects were investigated. Simulations at two axial heights above the inlet were compared to the experimental measurements of Rampure et al. [1] for a cylindrical bubble column. From previous FLUENT simulations [2], finer grid resolutions were not possible if the cell size was smaller than the bubble diameter. On the other hand, the CFDLib simulations produced grid-independent solutions at finer grid resolutions. The solution is physical as compared with the simulation of FLUENT. Similarly, the Wang-VanderHeyden drag coefficient model predicted homogeneous gas holdup across the bubble column without using the bubble pressure model. The Schiller-Naumann model predicted high gas holdup regimes off-center at lower axial liquid heights. The Wang-VanderHeyden and Schiller-Naumann models compare qualitatively well with experiments at lower and higher axial liquid heights, respectively. In short, the CFDLib simulations provide physical and grid-independent predictions with the experiments as the grid resolution becomes finer with and without the bubble pressure model. The drag coefficient model also influences the accuracy of the CFD predictions when compared to experiments.

ACKNOWLEDGMENTS

The authors would like to thank the generous financial support from the U.S. Department of Agriculture, Grant no. 2004-34188-15067. Additional appreciation is extended to the High Performance Computing Center at Iowa State University for their computer and technical support.

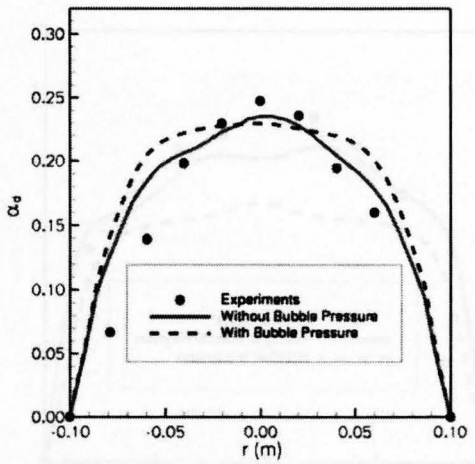

(a) 30 × 300 CELLS

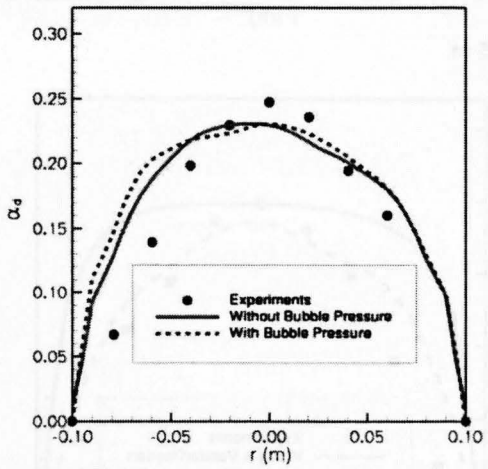

(b) 40 × 400 CELLS

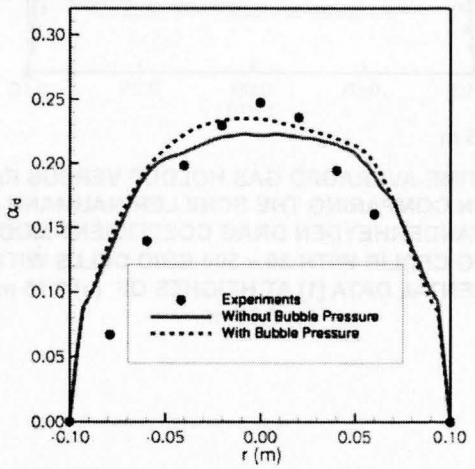

(c) 60 × 600 CELLS

Figure 6. TIME-AVERAGED GAS HOLDUP VERSUS RADIAL POSITION COMPARING CFDLIB SIMULATIONS WITH AND WITHOUT THE BUBBLE PRESSURE MODEL TO

EXPERIMENTAL DATA [1] AT A HEIGHT OF 0.65 M USING (a) 30 × 300, (b) 40 × 400 AND (c) 60 × 600 GRID CELLS.

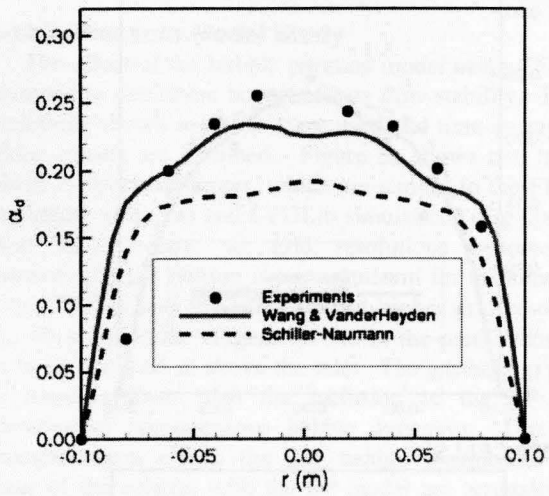

(a) H= 0.15 m

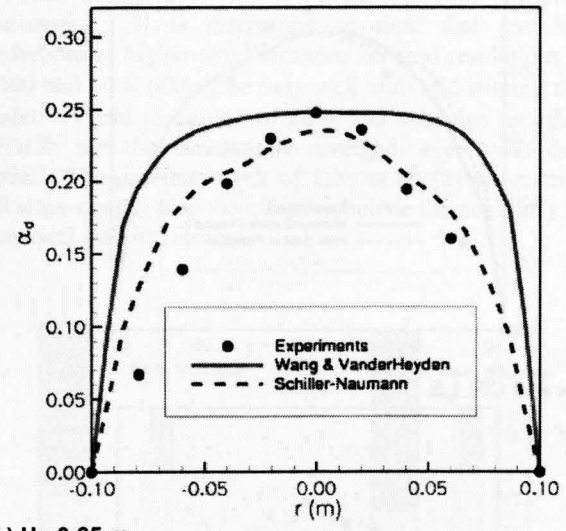

(b) H= 0.65 m

Figure 7. TIME-AVERAGED GAS HOLDUP VERSUS RADIAL POSITION COMPARING THE SCHILLER-NAUMANN AND WANG-VANDERHEYDEN DRAG COEFFICIENT MODELS USING CFDLIB WITH 30 × 300 GRID CELLS WITH EXPERIMENTAL DATA [1] AT HEIGHTS OF (a) 0.15 m AND (b) 0.65 m.

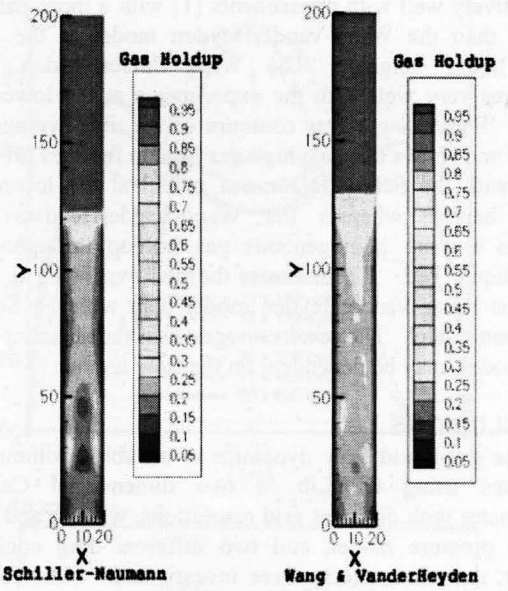

Figure 8. TIME-AVERAGED GAS HOLDUP CONTOUR PLOTS COMPARING THE SCHILLER-NAUMANN AND WANG-VANDERHEYDEN DRAG COEFFICIENT MODELS USING CFDLIB WITH 30 × 300 GRID CELLS.

REFERENCES

[1] Rampure, R.M., Buwa, V.V., Ranade, V.V., 2003, "Modeling of gas-liquid/gas-liquid-solid flows in bubble columns: Experiments and CFD Simulations", The Canadian Journal of Chemical Engineering, **81**, pp. 692-706.

[2] Law, D., Battaglia, F., and Heindel, T.J., 2006, "Numerical simulations of gas-liquid flow dynamics in bubble columns", Proceedings of the ASME Fluids Engineering Division, IMECE2006-13544, Chicago, IL.

[3] Sanyal, J., Vasquez, S., Roy, S., Dudukovic, M.P., 1999, "Numerical simulation of gas-liquid dynamics in cylindrical bubble column reactors", Chemical Engineering Science, **54**, pp. 5071-5083.

[4] Joshi, J.B., 2001, "Computational flow modeling and design of bubble column reactors", Chemical Engineering Science, **56 (21-22)**, pp. 5893-5933.

[5] Joshi, J.B., Vitankar, V.S., Kulkarni, A.A., Dhotre, M.T., Ekambara, K., 2002, "Coherent flow structures in bubble column reactors", **(57) 16**, pp. 3157-3183.

[6] Sokolichin, A., Eigenberger, G., 1994, "Gas-liquid flow in bubble columns and loop reactors: I. Detailed modeling and numerical simulation", Chemical Engineering Science, **49**, pp. 5735-5746.

[7] Pan, Y., Dudukovic, M.P., 2000, "Numerical investigation of gas-driven flow in 2-D bubble columns", Fluid Mechanics and Transport Phenomena, **46**, pp. 434-449.

[8] Monahan, S.M., Vitankar, V.S., Fox, R.O., 2005, "CFD predictions for flow-regime transitions in bubble columns", AIChE Journal, **51**, pp. 1897-1923.

[9] Delnoij, E., Lammers, F.A., Kuipers, J.A.M., van Swaaij, W.P.M., 1997a, "Dynamic simulation of dispersed gas-liquid two-phase flow using a discrete bubble model", Chemical Engineering Science, **52**(9), pp. 1429-1458.

[10] Delnoij, E., Kuipers, J.A.M., van Swaaij, W.P.M., 1997b, "Dynamic simulation of gas-liquid two-phase flow: effect of column aspect ratio on the flow structure", Chemical Engineering Science, **52**(21/22), pp. 3759-3772.

[11] Delnoij, E., Kuipers, J.A.M., van Swaaij, W.P.M., 1997c, "Computational fluid dynamics applied to gas-liquid contactors", Chemical Engineering Science, **52**(21/22), pp. 3623-3638.

[12] Lin, T-J., Reese, J., Hong, T., Fan, L.-S., 1996, "Quantitative analysis and computation of two-dimensional bubble columns", AIChE Journal, **42**, pp. 301-318.

[13] Hirt, C.W., Amsden, A.A., Cook, J.L., 1974, "An arbitrary Lagrangian-Eulerian computing method for all flow speeds", Journal of Computational Physics, **14**, pp. 227-253

[14] Launder, B.E., Spalding, D.B., 1974, "The numerical computation of turbulent flows", Computer Methods in Applied Mechanical Engineering, **3**, pp. 269-289.

[15] Kashiwa, B.A., VanderHeyden, W.B., 2000, "Toward a General Theory for Multiphase Turbulence", LA-13773-MS Report.

[16] Schiller, L., Naumann, Z., 1935, Z. Ver. Deutsch. Ing., pp.77-318.

[17] Kashiwa, B.A., Padial, N.T., Rauenzahn, R.M., VanderHeyden, W.B., 1994, "A cell-centered ICE method for multiphase flow simulations", Numerical Methods in Multiphase Flow, **185**, Proceedings of ASME Heat and Fluids Engineering Divisions (FED).

[18] Spelt, P.D.M., Sangani, A., 1998, "Properties and averaged equations for flows of bubbly liquids", Applied Science Reserve, **58**, pp. 337-386

[19] Biesheuvel, A., Gorissen, W.C.M., 1990, "Void fraction disturbances in a uniform bubbly fluid", International Journal of Multiphase Flow", **16**, pp. 211-231.